Supplemental Note 1:

We controlled for several factors that may confound model performance when models are fit to WT data and used to predict patterns in *bcd* RNAi. When building gene expression atlases, gene levels were normalized separately in each atlas, so changes in TF levels between genotypes are obscured. In WT, the gap genes express at similar levels {Little et al., 2013, #7748}, but their relative levels may be different in *bcd* RNAi. We controlled for this possibility in several ways. First, to simulate changes in level between genotypes, we systematically scaled the levels of each gene in *bcd* RNAi, one at a time, and measured model performance. For the pattern driven by the *eve3+7* reporter, the linear model was more accurate than the quadratic model for all tested scalings of *hb* and a very large range of scalings of the other regulators (Fig. S4). Analogously, for the endogenous pattern, the quadratic model always outperformed the linear model as we scaled *kni* and *tll* levels (Fig. S4). For *hb*, the quadratic model was more accurate than the linear model so long as *hb* levels in *bcd* RNAi were less than 135% of WT (Fig. S4). Since *hb* levels are reduced in *bcd* mutant embryos {Driever and Nüsslein-Volhard, 1989, #6801}, *hb* levels in *bcd* RNAi are almost certainly below this level. Second, we refit the models in *bcd* RNAi and predicted *bcd* RNAi output patterns, testing if an optimal set of parameters could change the relative predictive performance of the models, but it did not for T=3-6 (Fig. S5). Third, when we refit the models on both datasets simultaneously and predicted *bcd* RNAi patterns, the relative order of model performance did not change for T=3-6 (Fig. S5).

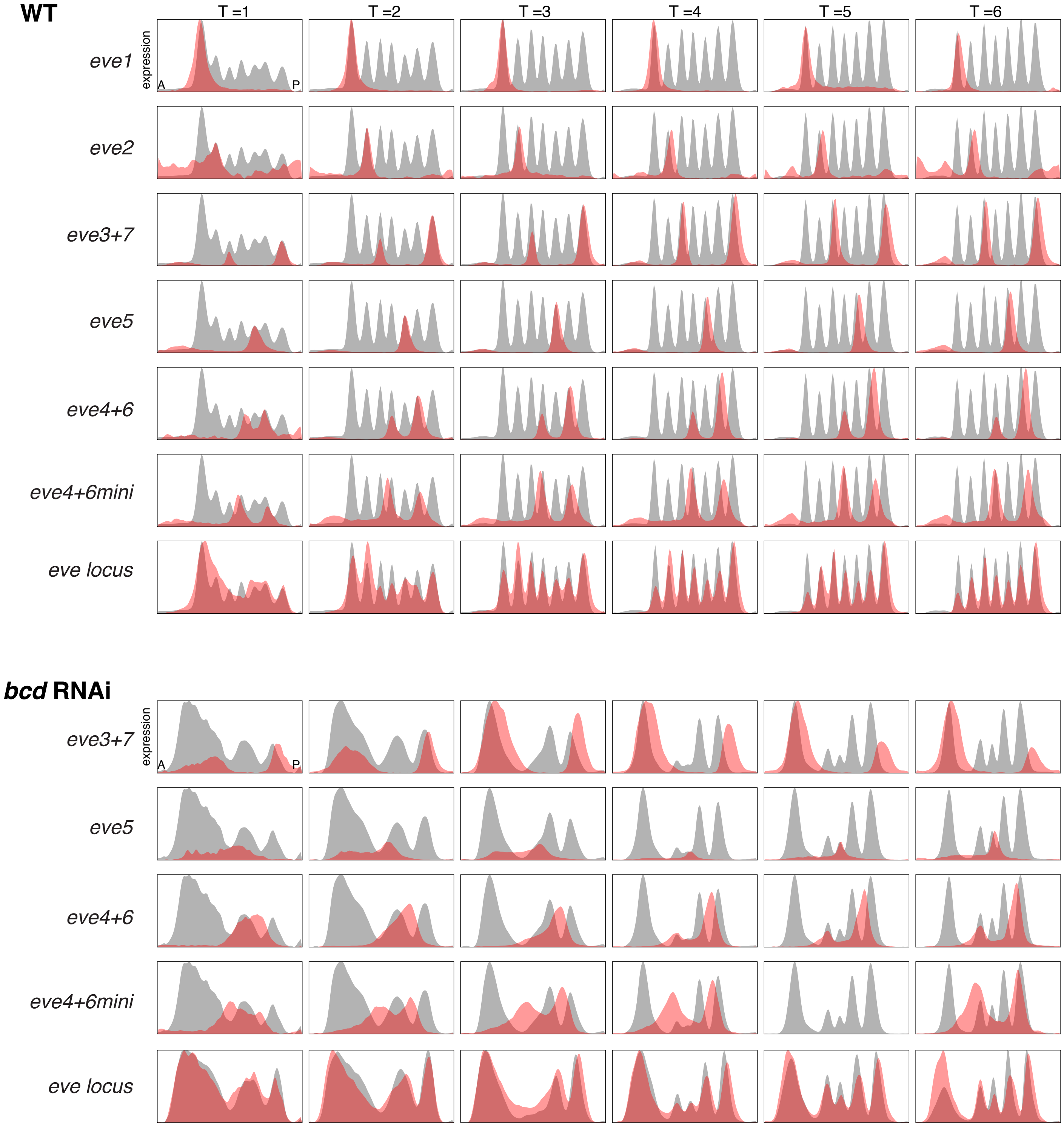

Figure S1: The isolated *eve* enhancer *lacZ* reporters overlap the corresponding endogenous patterns with varying fidelity.
Line traces of *lacZ* enhancer reporters (red) and the endogenous *eve* (gray) mRNA pattern in WT and *bcd* RNAi gene expression atlases. Anterior-posterior position (A-P) is plotted on the X-axis and expression level on the Y-axis for a lateral strip of the embryo.

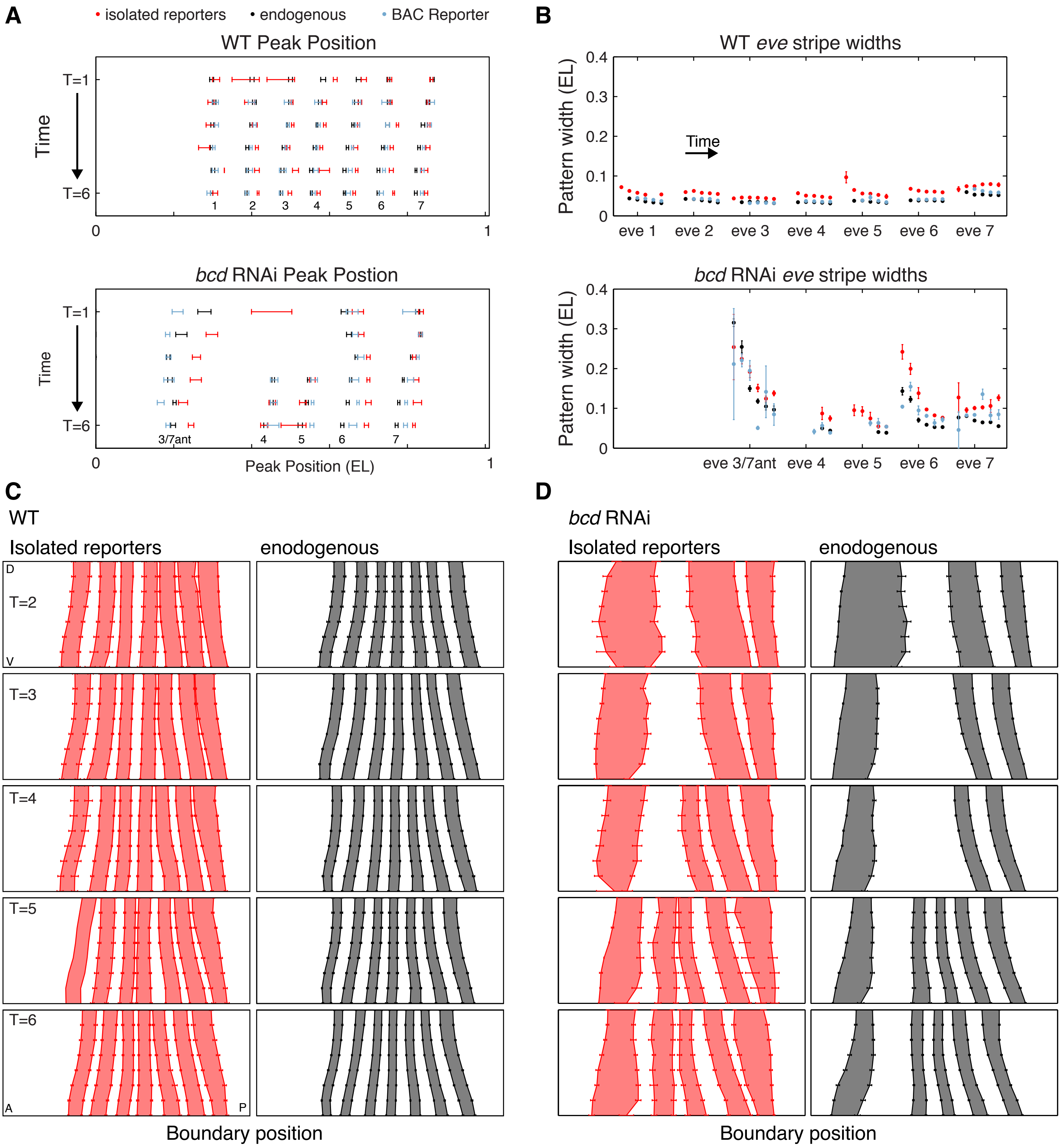

Figure S2: The expression pattern driven by the whole locus BAC reporter is nearly identical to the endogenous pattern, while the patterns driven by isolated reporters differ

(A) The reporter peak positions (red) are slightly posterior to the endogenous eve peaks (black) and BAC reporter peaks (blue). Peak positions in WT and *bcd* RNAi are calculated from the lateral line traces shown in Figure 2–figure supplement 1. The anterior *eve3+7* pattern is faint and broad at T=1 and the peak is close to the middle of the embryo as seen in the lateral line trace in Figure 2–figure supplement 1. **(B)** Stripe driven by the isolated reporters (red) are wider than endogenous stripes (black) and BAC reporter (blue) in WT and *bcd* RNAi. Widths are calculated from the lateral line traces shown in Figure 2–figure supplement 1. In WT, many of the errorbars are smaller than the diameter of the point. **(C-D)** Boundary positions of the isloated reporters (dark blue) and endogenous stripes (light blue) in WT (C) and *bcd* RNAi (D). Note, the ventral most part of the *eve3+7* reporter anterior pattern is very faint in *bcd* RNAi embryos and the analysis software does not reliably detect the position of this boundary.

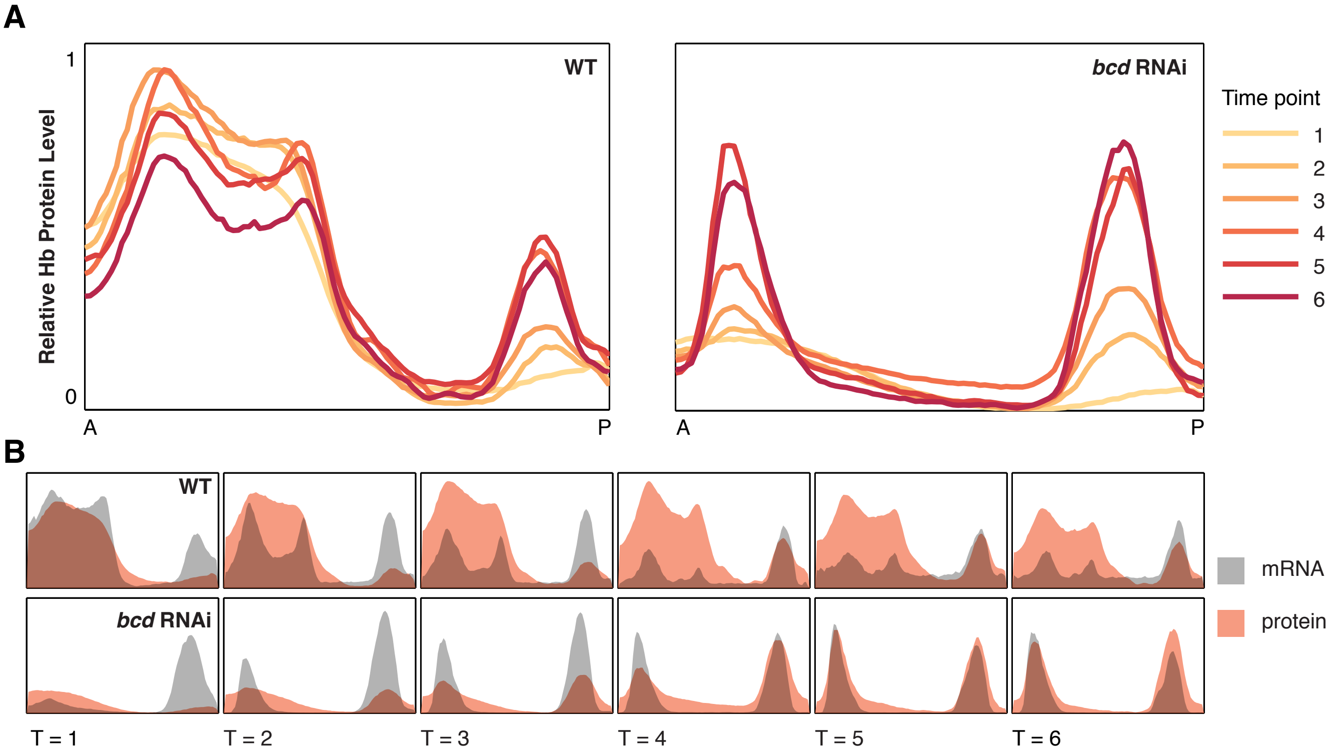

Figure S3: The *bcd* RNAi gene expression atlas perturbs *hb* mRNA and protein levels.
(A) *hb* protein expression pattern changes over stage 5 in both WT and *bcd* RNAi. In WT both maternal and *bcd* activated zygotic mRNA contribute to the anterior pattern, while in *bcd* RNAi, only maternal mRNA contributes {Tautz, 1988, #2648}. Note each atlas is normalized separately, so abosulte levels are not comparable between atlases. Relative levels change extensively.
(B) In both WT and *bcd* RNAi, *hb* mRNA (gray) and protein (red) patterns are different.

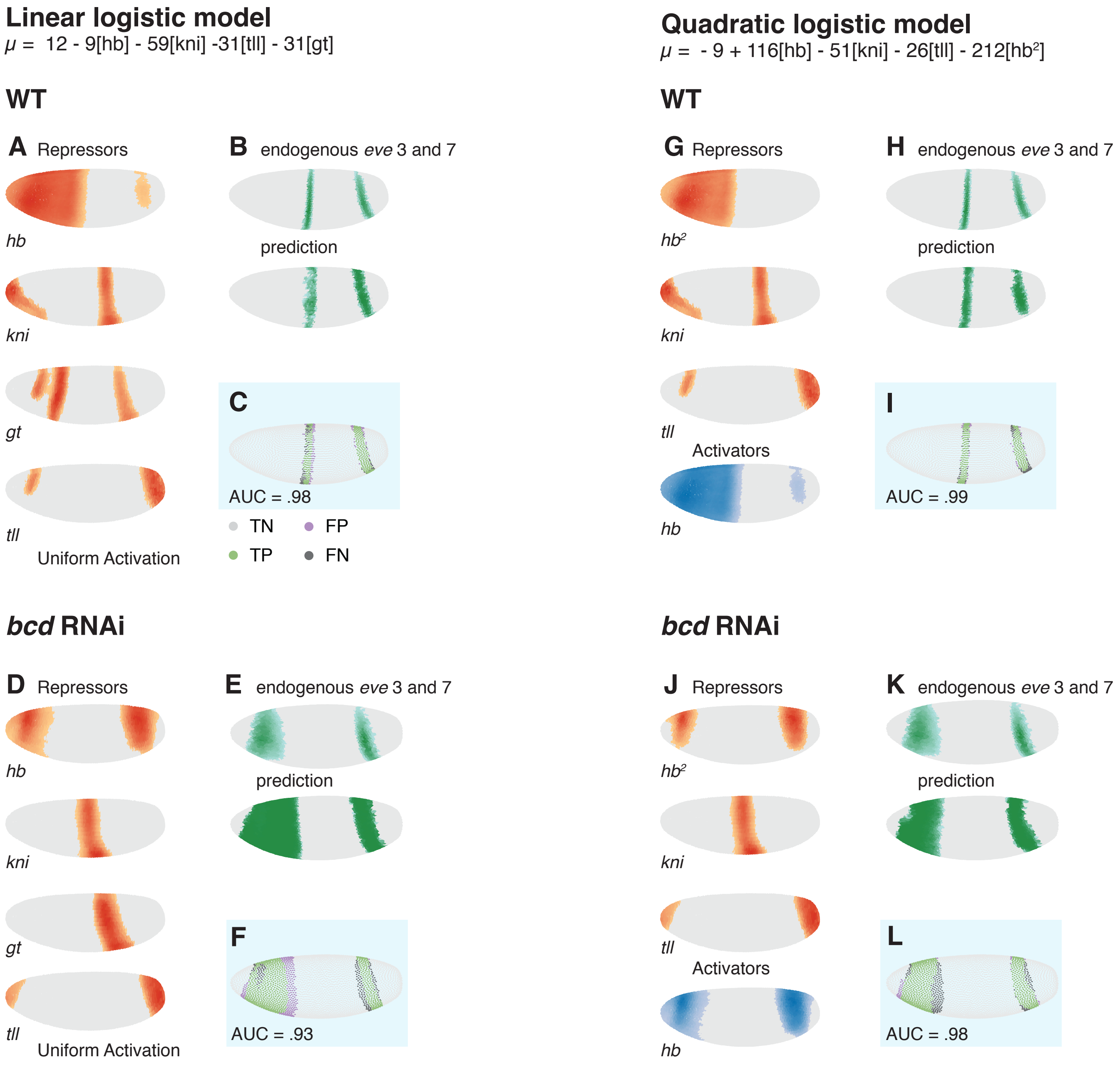

Figure S4: Under perturbation of *bcd,* the expression patterns of endogenous *eve* stripes 3 and 7 are more accurately predicted by the quadratic model.
(A) WT expression patterns of the regulators in the linear model. The expression level of each TF is shown for every cell. Cells with expression below an ON/OFF threshold (methods) are plotted in gray. For cells above this threshold, color intensity represents expression level. Repressors are red and activators are blue. **(B)** The expression pattern of the endogenous *eve* stripes 3 and 7 and the predictions of the linear model in WT. **(C)** Comparison of predictions to measurement in WT embryos. Green cells are true positives (TP), purple cells are false positives (FP), dark gray cells are false negatives (FN), and light gray cells are true negatives (TN). For visualization, the ON/OFF threshold is set to 80% sensitivity. The AUC metric quantifies performance over all thresholds. **(D)** The expression patterns of the regulators in the linear model in *bcd* RNAi embryos. **(E)** The expression pattern of the endogenous *eve* stripes 3 and 7 and the predictions of the linear model in *bcd* RNAi. **(F)** Comparison of linear model predictions to data in *bcd* RNAi. **(G-L)** Same as A-F, respectively, for the quadratic model.

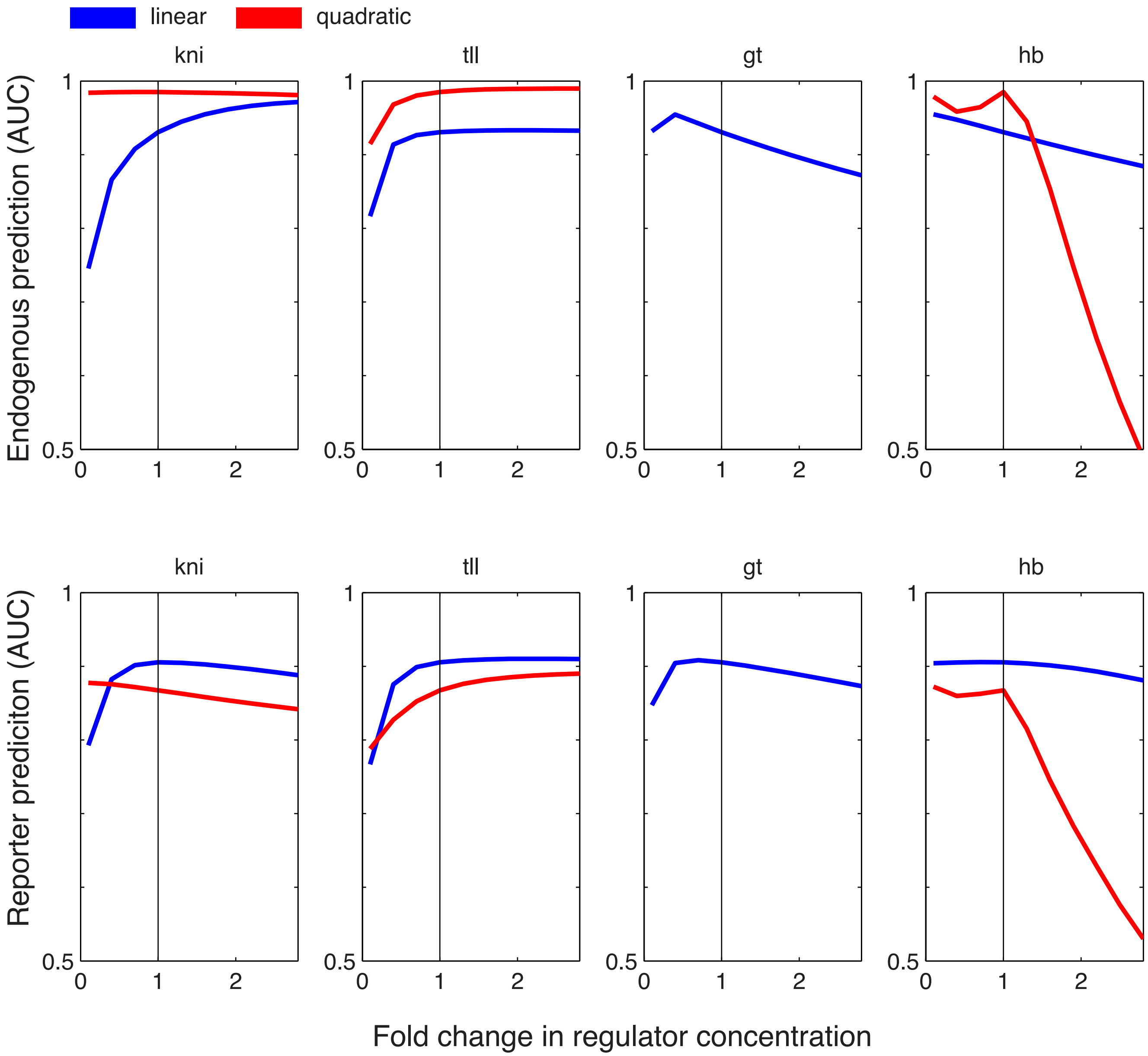

Figure S5: Sensitivity analysis shows that scaling the relative level of a TF between atlases generally does not change the relative performance of the models.
We varied the concentration of each TF separately in the *bcd* RNAi atlas and recalculated the AUC of the linear and quadratic models. This scaling simulates possible global changes in levels between genotypes.
For the endogeous pattern, for all scalings of *kni* and *tll* , the quadratic model is more accurate than the linear model. For *hb,* the quadratic model is more accurate than the linear model so long as maximal *hb* levels in *bcd* RNAi are less than 1.38x maximal WT levels. Since *bcd* is a potent activator of *hb, hb* levels are very likely reduced in *bcd* RNAi embryos.
For the reproter pattern, all scalings of *hb* preserve relative model accuracy. The linear model is more accurate for a broad scaling of *kni* and *tll* levels.

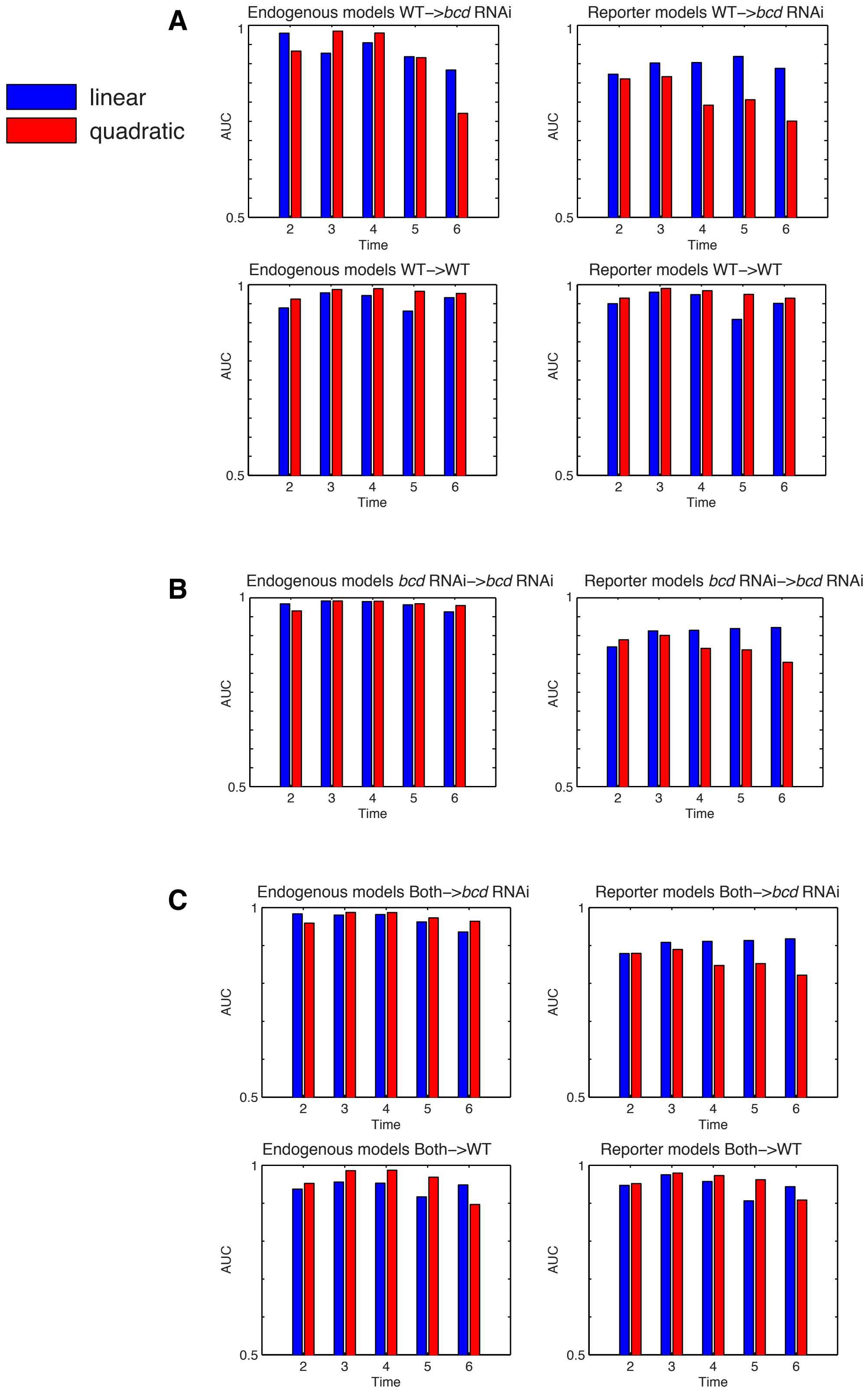

Figure S6: Fitting the linear and quadratic models on different datasets yielded similar results
(A) Fitting the models in WT at different time points and predicting the corresponding time points. The linear model always more accurately predicted the reporter *bcd* RNAi. Although both models are very accurate in WT, the quadratic model is more accurate. **(B)** Fitting the models in bcd RNAi and predicting *bcd* RNAi. The linear model more accurately predicted the reporter pattern. For the endogenous pattern, both models perfromed well. **(C)** Fitting the models on both the WT and *bcd* RNAi datasets led to similar results: the quadratic model more accurately predicted the endogenous pattern and the linear model more accurately predicted the reporter pattern in *bcd* RNAi.

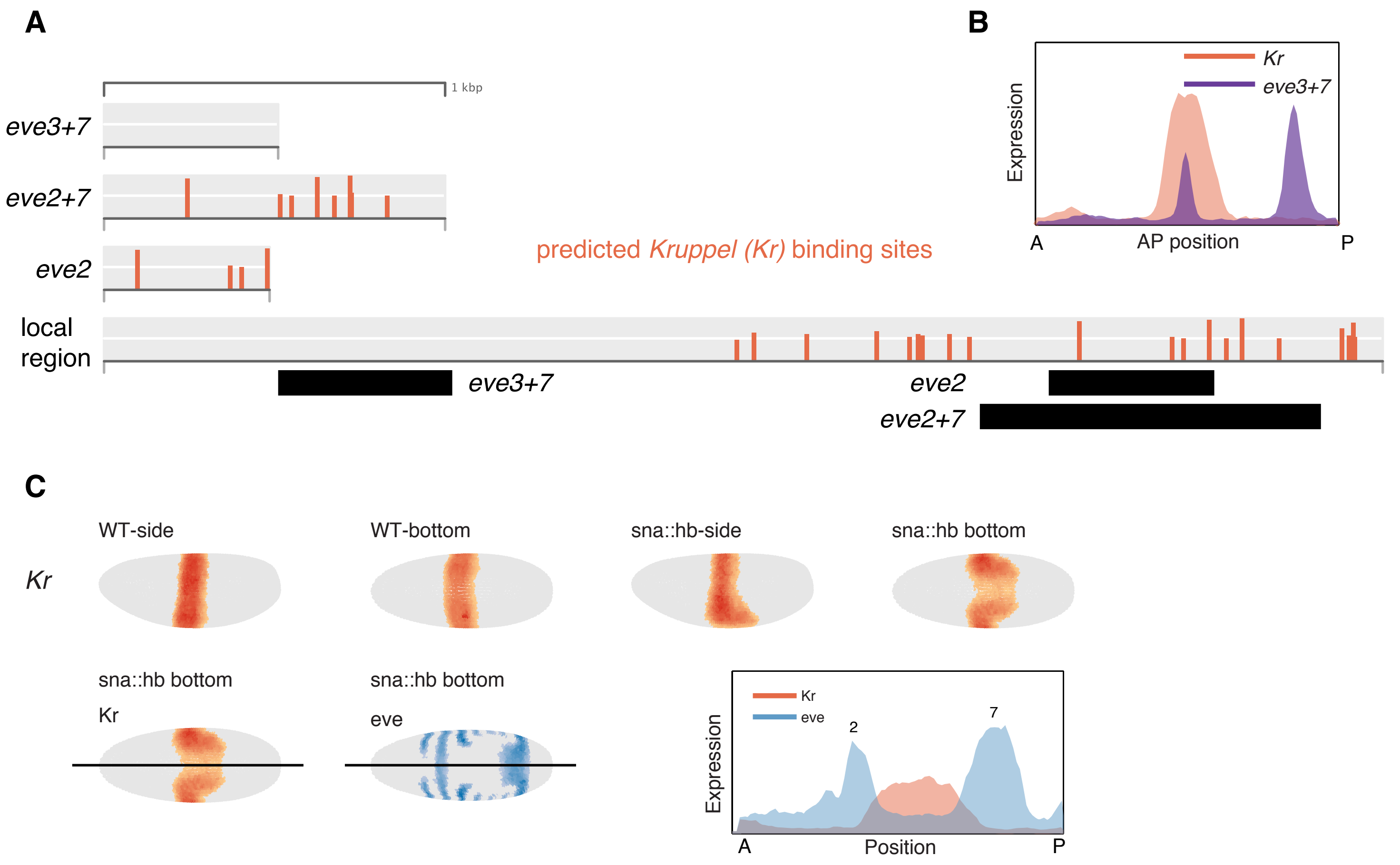

Figure S7: The expansion of the *Kr* expression pattern potentially explains the shape of the *eve2+7* expression pattern in *sna::hb* embryos
(A) The *eve2* enhancer is enriched for predicted *Kr* binding sites (red) while the *eve3+7* enhancer is depleted for *Kr* binding sites. We predicted binding sites using PATSER (stormo.wustl.edu) with a position weight matrix derived from bacterial 1-hybrid data (Noyes et al., 2008). **(B)** *Kr* expression overlaps stripe 3 of the *eve3+7* reporter mRNA in WT. *Kr* does not repress this pattern consistend with the absence of binding sites. **(C)** The distribution of *Kr* mRNA in WT and *sna::hb* misexpression embryos. The expanded ventral region of the *Kr* mRNA pattern appears to set the boundary of the expanded endogenous *eve* stripe 7 pattern.

Model Parameters

		Linear						**Quad**				
	Time	**const**	***hb***	***kni***	***tll***	***gt***		**const**	***hb***	***kni***	***tll***	***hb*^{2}**
Endogenous	**2**	5	-5	-21	-9	-15		-5	68	-22	-7	-134
hb protein	3	12	-9	-59	-31	-31		-9	116	-51	-26	-212
others mRNA	**4**	11	-5	-40	-51	-27		-9	101	-42	-67	-137
	5	5	-2	-17	-25	-14		-7	73	-26	-49	-95
	6	10	-4	-48	-37	-33		2	49	-50	-58	-77
Endogenous	3	12	-9	-59	-31	-31		-9	116	-51	-26	-212
Ilsley et al. 2013 (includes gt protein)	**3**	11	-10	-66	-22	-13		-8	110	-45	-25	-201
		Linear						**Quad**				
	Time	**const**	***hb***	***kni***	***tll***	***gt***		**const**	***hb***	***kni***	***tll***	***hb*^{2}**
Reporter	**2**	6	-6	-30	-6	-16		-3	64	-37	-4	-134
hb protein	**3**	12	-11	-72	-18	-29		-10	145	-73	-14	-286
others mRNA	**4**	11	-7	-37	-22	-43		-13	105	-25	-16	-144
	5	4	-1	-13	-14	-15		-12	83	-15	-22	-103
	6	8	-4	-26	-22	-40		-5	59	-19	-23	-91

AUC scores

	Linear		**Quadratic**	
T = 3	**Ilsley et al. 2013**	**Refit**	**Ilsley et al. 2013**	**Refit**
WT	0.9622	0.9786	0.9874	0.9874
bcd RNAi	0.9321	0.9275	0.9850	0.9849

Table S1: Model parameters

Construct	Enhancer sequence	Reference	Primer sequences
eve1	AGGCCTAATCACTTCCCTGAAATGCATAATTGTGCCGCGGCTTTTGATACGCTCCTGGCGGAGAGGGAGATGAGGAAAGGATGCACGGGAACCGCAGCCAAGTGGCAGTCGAGATTGGCAAATCCGCCAGCGGACAATGCCCAGAGAATGGGCAACAAGTAGCGGCGAATTAGCAATCCTATCATGCTTTTATGGCCGGCCAACTCTTGCCCGCGCATCTCAGTTCATCCGAAGCGGGACCAGGTCCAGGTTCAAGTCGAGGTCCAGTACCCCTGCTATCCCGTCAACCCCTTTAGGGCGATAATCCTTCTAAATGTTTGCATTAATTTCGAGGCGTGGACGGATTAGGGCGTGCTGGCTGGGCGGAACCCGCAGCAGAAACCGCCGAGGACACTGCACCGACTGACCTGCAGCCTACAGATCTCTGATCTTCGATCTCTAATCCTTTCGCATTTGCAACTGACTTCTGCACTGGGTCCGCCCCTAATCCTTCCGCCGAGAAGGCGGCAGAGTCGCGAGGTACTGGCCCGGGGTAATGGGATTATCTGCGATTACCCCAGATGATCCGCAGAAAGTCAATCTGGTTCAGGGGCTAATTGTCAGCGAAGTCAACTAAATCCAATCCTTTCGCGCCCCCTTCTGTTTATTTGTTTGTTTTCGTTTGTTTTGAGAATTTCTGGCAATTAAGTTGCCCGTTTTGATGCGCGGGGGCGGGTGCATCAAATCCTTTCGGCATACCTGTCCTGCACAAATGCTGAATTCCGCATCCCATGGATACCCAGATATTCAGATATCCCAAGGC	Fujioka et al., 1999	AGGCCTAATCACTTCCCTG
			GCCTTGGGATATCTGAATATCTGG
eve4+6	AGGATCCCTGGGCTCTGGGCTCTGGACTATCCGCCGACCCTCCATATCCATGATTTACAATTCTCGTTTTTTTCGCGTTATTTTTTTAGGGGCTTTAATGACCGTCGTAAAGCCGCAGGAGGACCAGGACCAGGACTCTGCTCACATTTCGCGCACTGATTCTAAAAAATGAAATCATTTTTTCTTGAATTTCACGGCGCGCCTCGAGCAGGACTCTTTGTTCTCGGCCAGGCAATTGTCCTTTTTTGCGCTCAGCTCTCAGTTTTTTCGTCCAGCGGGCATTACCTACACGGCGTTTTATGGCGGAGATGATATTCGCCTGGGATCGGTTCCGTTTTTTAGGCCATAAAAATTAGGCGGCATAAAAAAACTGCATTGGAATTCTAGTTCTAGTTTCAAGTTTTTAGGTTTCCAGGTTTCTGCCAGCCCGCCTAGATTCGCATTTCGCGGAATTCGGAAGCGGAACAGAATGCCAGAATGGTCAGAATCCTGGCTGACCTTGCCTTTTGGCCAGGGGCCGTAAAAAAATTGACTCGCTGCGGTGCGCGGAATATTTTTTAAATCTGACTTTCCAACAATCTCTGATCTGGGTTCGAATCGTAAAAAAAAAGCAGAACAAAAAGCGGGCATTTTCGTCGGCAAATGATCTGTTAATGGGCCGGGCTAAAAAACTAAGTCACAAAGTCACAAGGTTGTCCGGTAAATTGACCCGGTTAAGAATGTCTGTCTGTACCGAGAAGGATGCAGGACATTCAGCACTTCAAAGCTCCCACCGCTCGAAGGATTCCCCCGAAGATTCAC	Fujioka et al. 1999	AGGATCCCTGGGCTCTG
			GTGAATCTTCGGGGGAATCC
eve5	ATATCCCAAGGCCGCAAAGTCAACAAGTCGGCAGCAAATTTCCCTTTGTCCGGCGATGTGTTTTTTTTTAGCCATAACTCGCTGCATTGTTTGGGCCAAGTTTTTCTTCTGCCAAATTGCGGAGATGATGCGGGGATTATGCGCTGATTGCGTGCAATTATGGACATCCTGCGAGGCCCCGAGGAACTTCCTGCTAAATCCTTTCATCCGCCTACAGAACCCCTTTGTGTCCCGTTCGCCGGGAGTCCTTGACGGGTCCTTCGACTATTCGCTTACAGCAGCTTGCGTAAAATTTCATAACCCTACGAGCGGCTCTTCCGCGGAATCCCTGGCATTATCCTTTTTACCTCTTGCCAATCCGTTGGCTAAAAAACGGCTTCGACTTCCGCGTAACTGCTGGACAACAAAGACAAAAAACGGCGAAAGGACGGCGATTTCCAGGTAGCATTGCGAATTCCGTCAAACTAAAGGACCGGTTATATAACGGGTTTATATGGCCAGAATCTCTGCATCTCCACGACCGCCAGAAGCTGCGTAAAACTGCAGGCTCTGTTTTGATTTCTGCAACTTCAGTTAATTGCCCGGGATGGCCAGCAATTGCCGGCAATTATAAAACAGCGCAGATGTGACTCAGCTTCCATATCTAACTCTATATCTCATGCCGAAAATCTAGGGTGGGGAGCGGAGGGGCGGGGTGCGTGGGTGACTTGCCTGCCAGGGAAAGGGGGCGGGGGTTCAGCGGGTGATAAATGTGCGTGATTTGGAATGAATGCGCATCGATTAAAACCGCAGGGCAATCAATTT	Fujioka et al. 1999	ATATCCCAAGGCCGCAAAG
			AAATTGATTGCCCTGCGGT
eve3+7	GGATCCTCGAAATCGAGAGCGACCTCGCTGCATTAGAAAACTAGATCAGTTTTTTGTTTTGGCCGACCGATTTTTGTGCCCGGTGCTCTCTTTACGGTTTATGGCCGCGTTCCCATTTCCCAGCTTCTTTGTTCCGGGCTCAGAAATCTGTATGGAATTATGGTATATGCAGATTTTTATGGGTCCCGGCGATCCGGTTCGCGGAACGGGAGTGTCCTGCCGCGAGAGGTCCTCGCCGGCGATCCTTGTCGCCCGTATTAGGAAAGTAGATCACGTTTTTTGTTCCCATTGTGCGCTTTTTTCGCTGCGCTAGTTTTTTTCCCCGAACCCAGCGAACTGCTCTAATTTTTTAATTCTTCACGGCTTTTCATTGGGCTCCTGGAAAAACGCGGACAAGGTTATAACGCTCTACTTACCTGCAATTGTGGCCATAACTCGCACTGCTCTCGTTTTTAAGATCCGTTTGTTTGTGTTTGTTTGTCCGCGATGGCATTCACGTTTTTACGAGCTC	Small et al., 1996	GGATCCTCGAAATCGAGAGC
			GAGCTCGTAAAAACGTGAATGC
eve2	GGTTACCCGGTACTGCATAACAATGGAACCCGAACCGTAACTGGGACAGATCGAAAAGCTGGCCTGGTTTCTCGCTGTGTGTGCCGTGTTAATCCGTTTGCCATCAGCGAGATTATTAGTCAATTGCAGTTGCAGCGTTTCGCTTTCGTCCTCGTTTCACTTTCGAGTTAGACTTTATTGCAGCATCTTGAACAATCGTCGCAGTTTGGTAACACGCTGTGCCATACTTTCATTTAGACGGAATCGAGGGACCCTGGACTATAATCGCACAACGAGACCGGGTTGCGAAGTCAGGGCATTCCGCCGATCTAGCCATCGCCATCTTCTGCGGGCGTTTGTTTGTTTGTTTGCTGGGATTAGCCAAGGGCTTGACTTGGAATCCAATCCCGATCCCTAGCCCGATCCCAATCCCAATCCCAATCCCTTGTCCTTTTCATTAGAAAGTCATAAAAACACATAATAATGATGTCGAAGGGATTAGGGG	Small et al., 1991	GGTTACCCGGTACTGCATAAC
			CCCCTAATCCCTTCGACATC
eve2+7	AGAAGGCTTGCATGTGGGCCTTTTCCAGGTCGGCCAGTAGGTAGAGTTGTTGCGATGCGGCTATGCCGGGCGAGTTAATGCCAATGCAAATTGCGGGCGCAATATAACCCAATAATTTGAAGTAACTGGCAGGAGCGAGGTATCCTTCCTGGTTACCCGGTACTGCATAACAATGGAACCCGAACCGTAACTGGGACAGATCGAAAAGCTGGCCTGGTTTCTCGCTGTGTGTGCCGTGTTAATCCGTTTGCCATCAGCGAGATTATTAGTCAATTGCAGTTGCAGCGTTTCGCTTTCGTCCTCGTTTCACTTTCGAGTTAGACTTTATTGCAGCATCTTGAACAATCGTCGCAGTTTGGTAACACGCTGTGCCATACTTTCATTTAGACGGAATCGAGGGACCCTGGACTATAATCGCACAACGAGACCGGGTTGCGAAGTCAGGGCATTCCGCCGATCTAGCCATCGCCATCTTCTGCGGGCGTTTGTTTGTTTGTTTGCTGGGATTAGCCAAGGGCTTGACTTGGAATCCAATCCTGATCCCTAGCCCGATCCCAATCCCAATCCCTTGTCCTTTTCATTAGAAAGTCATAAAAACACATAATAATGATGTCGAAGGGATTAGGGGCGCGCAGGTCCAGGCAACGCAATTAACGGACTAGCGAACTGGGTTATTTTTTTGCGCCGACTTAGCCCTGATCCGCGAGCTTAACCCGTTTTGAGCCGGGCAGCAGGTAGTTGTGGGTGGACCCCACGATTTTTTTGGCCAAACCTCCAAGCTAACTTGCGCAAGTGGCAAGTGGCCGGTTTGCTGGCCCAAAAGAGGAGGCACTATCCCGGTCCTGGTACAGTTGGTACGCTGGGAATGATTATATCATCATAATAAATGTTTTGCCCAACGAAACCGAAAACTTTTCAAATTAAGTCCCGGCAACTGGGTTCCCATTTTCCATTTTCCATGTTCTGCGGGCAGGGGCGGCCATTATCTCGCT	this work	AGAAGGCTTGCATGTGGG
			AGCGAGATAATGGCCGCC
BAC whole locus	Beginning -6.4 kb upstream of *eve* transcription start site (TSS) and ending 11.3 kb downstream of *eve* TSS. The *eve* coding sequence has been replaced with *LacZ* and the neighboring *TER94* gene has been fused to GFP	Gift from M. Fujioka	

Table S2: Enhancer reporter sequences and primers used to generate them.

The *eve2+7* enhancer spans 998 bp including the entire minimal *eve2* enhancer, but none of the *eve3+7* enhancer (Fig. S6). Late in this work, we noticed this construct had a 1 bp polymorphism and a 6 bp deletion in the minimal *eve2* region, but neither of these defects affects any of the foot-printed binding sites (Small et al., 1991; Small et al., 1992).